Iron Phosphinimide and Phosphinimine Complexes: Catalyst Precursors for Ethylene Polymerization

Luc LePichon,† Douglas W. Stephan,*,† Xiaoliang Gao,‡ and Qinyan Wang‡

School of Physical Sciences, Chemistry and Biochemistry, University of Windsor, Windsor, Ontario, Canada N9B 3P4, and NOVA Chemicals Corporation, Research & Technology Center, 2928 16 Street N.E, Calgary, Alberta, Canada T2E 7K7

Received December 6, 2001

Reaction of Li[NP*t*-Bu$_3$] with FeCl$_2$ affords [Cl$_3$Fe$_2$(μ-NP*t*-Bu$_3$)$_2$] **1** in 71% yield. This mixed valent Fe(III)−Fe(II) undergoes reversibly one-electron oxidation to generate [Cl$_3$Fe$_2$(μ-NP*t*-Bu$_3$)$_2$]$^+$. Chemical oxidation with [Cp$_2$Fe]PF$_6$ yields [Cl$_2$Fe(μ-NP*t*-Bu$_3$)]$_2$ **2**. The reaction of Li[NP*t*-Bu$_3$] with FeBr$_3$ affords [Br$_4$Fe$_2$(μ-NP*t*-Bu$_3$)$_2$] **3**, while the reaction of FeCl$_3$ with Me$_3$SiNPCy$_3$ gives [Cl$_2$Fe(μ-NPCy$_3$)]$_2$ **4**. Hydrolysis of **3** yields the species [(*t*-Bu$_3$PNH)Br$_2$Fe]$_2$(μ-O) **5**. These species have also been evaluated as catalysts for the polymerization of ethylene and copolymerization of ethylene/octene. These species were found to be single-site catalysts even under rather demanding conditions (50−160 °C, 100−300 psig ethylene), although the activities are generally low. Compound **5** affords polymer similar to that produced by **3**, suggesting that MAO dehydrates **5** generating a catalyst similar to that derived from **3**. Compounds **1**, **2**, **4**, and **5** have been crystallographically characterized.

The impact of plastics and polymers on modern society continues to spur the exploration of transition metal complexes for single-site olefin polymerization catalysts. These efforts have resulted in the evolution from early metal metallocenes[1,2] to early metal nonmetallocenes[3] and Schiff base−late metal catalyst systems.[4−12] In our work, we have recently reported the use of sterically demanding phosphinimide ligands in the development of nonmetallocene, titanium-based ethylene polymerization catalysts.[13,14] In this regard, we have developed remarkably active polymerization catalysts derived from the species (*t*-Bu$_3$PN)$_2$TiR$_2$.[13] Of particular recent interest are developments of late metal olefin polymerization catalysts by the research groups of Brookhart,[5,6,15] Gibson,[7−9,16] and most recently Grubbs.[11] Such systems are extremely interesting, as they offer a unique approach to a variety of branched polyolefins. While such catalysts are thought to be deactivated by moisture and oxygen, they do offer the potential of greater functional group tolerance than group IV systems. In continuing our efforts, we are exploring late metal complexes of both phosphinimide and phosphinimine ligands. In this work we explore the utility of Fe-phosphinimide complexes as precursors for olefin polymerization catalysts.

Experimental Section

General Data. All preparations were done under an atmosphere of dry, O_2-free N_2 employing both Schlenk line techniques and an Innovative Technologies or Vacuum Atmospheres inert atmosphere glovebox. Solvents were purified employing a Grubb's type column system manufactured by Innovative Technology. All organic reagents were purified by conventional methods. Guelph Chemical Laboratories, Guelph, Ontario, performed combustion analyses.

Synthesis of [Cl$_3$Fe$_2$(μ-NP*t*-Bu$_3$)$_2$] 1. Li[NP*t*-Bu$_3$] (446 mg, 2.00 mM) in THF solution (40 mL) was added to a suspension of FeCl$_2$ (254 mg, 2.00 mM) in 10 mL of THF. The reaction mixture was stirred for 2 h at 25 °C, resulting in a gray powdery precipitate. The solvent was removed in vacuo, and 15 mL of CH_2Cl_2 was added. The dark red solution was stirred for 20 min and filtered through Celite, and the filtrate was concentrated. Dark red crystals of **1** crystallized from solution upon standing (71% yield). Anal. Calcd for $C_{24}H_{54}Cl_3Fe_2N_2P_2$: C, 44.30; H, 8.36; N, 4.30; Found: C, 43.36; H, 8.45; N, 4.21.

Synthesis of [Cl$_2$Fe(μ-NP*t*-Bu$_3$)]$_2$ 2. [Cp$_2$Fe]PF$_6$ (66 mg, 0.20 mM) was added to a solution of **1** (130 mg, 0.20 mM) in 10 mL of CH_2Cl_2. The solution was stirred 2 h at 25 °C. After filtration through Celite the solution was evaporated and the resulting red-brown powder washed with hexane. Recrystallization in CH_2Cl_2 afforded red-brown crystals of **2** in 90% yield

* Corresponding author. E-mail: stephan@uwindsor.ca.
† University of Windsor.
‡ NOVA Chemicals Corporation.

(1) Kaminsky, W. *J. Chem. Soc.* (*D*) **1998**, 1413−1418.
(2) Hlatky, G. G. *Coord. Chem. Rev.* **1999**, *181*, 243−296.
(3) Hlatky, G. G. *Coord. Chem. Rev.* **2000**, *199*, 235−329.
(4) Brookhart, M. *Organometallics* **2000**, *19*, 2125−2129.
(5) Small, B. L.; Brookhart, M.; Bennett, A. M. A. *J. Am. Chem. Soc.* **1998**, *120*, 4049−4050.
(6) Killian, C. M.; Tempel, D. J.; Johnson, L. K.; Brookhart, M. *J. Am. Chem. Soc.* **1996**, *118*, 11664−11665.
(7) Britovsek, G. J. P.; Gibson, V. C.; Wass, D. F. *Angew. Chem., Int. Ed.* **1999**, *38*, 428−447.
(8) Gibson, V. C.; Newton, C.; Redshaw, C.; Solan, G. A.; White, A. J. P.; Williams, D. J. *J. Chem. Soc.* (*D*) **1999**, 827−829.
(9) Britovsek, G. J. P.; Gibson, V. C.; Kimberley, B. S.; Maddox, P. J.; McTavish, S. J.; Solan, G. A.; White, A. J. P.; Williams, D. J. *Chem. Commun.* **1998**, *007*, 849−850.
(10) Coles, M. P.; Dalby, C. I.; Gibson, V. C.; Clegg, W.; Elsegood, M. R. J. *Chem. Commun.* **1995**, 1709−1712.
(11) Younkin, T. R.; Connor, E. F.; Henerson, J. I.; Friedrich, S. K.; Grubbs, R. H.; Bansleben, D. A. *Science* **2000**, *287*, 460−462.
(12) Theopold, K. H. *Eur. J. Inorg. Chem.* **1998**, 15−24.
(13) Stephan, D. W.; Guerin, F.; Spence, R. E. V. H.; Koch, L.; Gao, X.; Brown, S. J.; Swabey, J. W.; Wang, Q.; Xu, W.; Zoricak, P.; Harrison, D. G. *Organometallics* **1999**, *18*, 2046−2048.
(14) Stephan, D. W.; Stewart, J. C.; Guerin, F.; Spence, R. E. V. H.; Xu, W.; Harrison, D. G. *Organometallics* **1999**, *18*, 1116−1118.
(15) Johnson, L. K.; Killian, C. M.; Brookhart, M. *J. Am. Chem. Soc.* **1995**, *117*, 6414−6415.
(16) Gibson, V. C.; Marshall, E. L.; Redshaw, C.; Clegg, W.; Elsegood, M. R. J. *J. Chem. Soc.* (*D*) **1996**, 4197−4200.

10.1021/om011041m CCC: $22.00
Publication on Web 03/08/2002

Table 1. Crystallographic Parameters

	1	2	4	5
formula	$C_{24}H_{54}Cl_3Fe_2N_2P_2$	$C_{24}H_{54}Cl_4Fe_2N_2P_2$	$C_{36}H_{66}Cl_4Fe_2N_2P_2$	$C_{24}H_{56}Br_4Fe_2N_2OP_2$
fw	650.68	686.16	842.34	881.98
a (Å)	11.7067(15)	13.3445(3)	9.3084(3)	19.104(4)
b (Å)	12.7469(15)	16.4624(4)	16.2308(2)	15.719(2)
c (Å)	12.8426(17)	15.1202(3)	14.3609(4)	25.267(6)
α (deg)	65.577(2)			
β (deg)	76.774(2)		105.082(2)	
γ (deg)	69.131(3)			
cryst syst	triclinic	orthorhombic	monoclinic	orthorhombic
space group	*P*$\bar{1}$	*Pbcm*	$P2_1/c$	*Pbca*
vol (Å^3)	1623.0(4)	3321.64(13)	2094.95(9)	7588(2)
D_{calcd} (g cm^{-1})	1.331	1.372	1. 335	1.544
Z	2	4	2	8
abs coeff, μ (mm^{-1})	1.255	1.308	1.051	5.080
no. of data collected	3754	16 631	10 149	34 911
no. of data $F_o^2 > 3\sigma(F_o^2)$	2297	3043	3636	6678
no. of variables	298	166	208	315
R (%)	10.79	7.19	6.24	8.45
R_w (%)	25.69	17.89	10.39	17.93
goodness of fit	1.012	1.091	0.979	1.065

[a] All data collected at 24 °C with Mo Kα radiation ($\lambda = 0.71069$ Å), $R = \sum||F_o| - |F_c||/\sum|F_o|$, $R_w = [\sum[w(F_o^2 - F_c^2)^2]/\sum[wF_o^2)^2]]^{0.5}$.

(123 mg). Anal. Calcd for $C_{24}H_{54}Cl_4Fe_2N_2P_2 + 0.50CH_2Cl_2$: C, 40.39; H, 7.61; N, 3.84. Found: C, 40.49; H, 8.05; N, 3.83.

Synthesis of [Br$_2$Fe(*μ*-NP*t*-Bu$_3$)]$_2$ 3. A solution of Li[NP*t*-Bu$_3$] (2.86 mg, 1.3 mmol) in hexane was added to a suspension of $FeBr_3$ (385 mg, 1.3 mmol) in toluene (40 mL) at −30 °C. The mixture was slowly warmed to room temperature with stirring for 12 h. The brownish-orange solution was filtered and concentrated, heptane was added, and the reaction mixture was allowed to stand at −35 °C to give an orange crystalline product, **1** (540 mg, 96% yield). Anal. Calcd for $C_{24}H_{54}Br_4Fe_2N_2P_2$: C, 33.36; H, 6.30; N, 3.24. Found: C, 33.09; H, 6.00; N, 2.97.

Synthesis of [Cl$_2$Fe(*μ*-NPCy$_3$)]$_2$ 4. A solution of $FeCl_3$ (91 mg, 0.56 mM) and $Cy_3PNSiMe_3$ (620 mg, 1.69 mM) in 10 mL of dichloroethane was stirred at reflux during 4 h. After evaporation of the solution the resulting red-brown powder was washed with hexane. Recrystallization in CH_2Cl_2 afforded red-brown crystals of **4** in relatively low yield (20%). Anal. Calcd for $C_{36}H_{66}Cl_4Fe_2N_2P_2$: C, 51.33; H, 7.90; N, 3.33. Found: C, 51.01; H, 7.30; N, 2.92.

Synthesis of [BrFe(HNP*t*-Bu$_3$)]$_2$(*μ*-O) 5. A solution of LiNP*t*-Bu$_3$ (406 mg, 1.9 mmol) was suspended in anhydrous heptane (20 mL). $FeBr_3$ (552 mg, 1.9 mmol) was dissolved in toluene (30 mL) and added to the heptane solution at −100 °C. The solution was stirred and warmed to room temperature and H_2O (16 mg, 0.88 mmol) was added dropwise in a toluene (60 mL) solution. The mixture was stirred for 12 h, the solution filtered, and the solvent removed. The light green product was washed with heptanes, affording **5** in 34% yield. Anal. Calcd for $C_{24}H_{56}Br_4Fe_2N_2P_2O$: C, 32.68; H, 6.40; N, 3.18. Found: C, 32.21; H, 6.30; N, 2.97.

Ethylene Polymerization. These experiments were done in one of two ways. Each are described below. (i) A solution of 6−10 *μ*mol of catalyst precursor in 2.0 mL of dry toluene was added to a flask containing 2.0 mL of dry toluene. Five hundred equivalents of a 10 wt % toluene solution of methylaluminoxane (MAO) was added to the flask. Alternatively, a catalyst precursor was combined with $[Ph_3C][B(C_6F_5)_4]$ under an ethylene atmosphere. The flask was attached to a Schlenk line with a cold trap, a stopwatch was started, and the flask was three times evacuated for 5 s and refilled with predried 99.9% ethylene gas. The solution was rapidly stirred under 1 atm of ethylene at room temperature. The polymerization was stopped by the injection of a 1.0 N HCl/methanol solution, total reaction time was noted, and the polymer was isolated. (ii) A 1 L autoclave was dried under vacuum (10^{-2} mmHg) for several hours. Dried toluene (500 mL) was transferred into the vessel under a positive pressure of N_2 and was heated to 30 °C. The temperature was controlled (to ca. ±2 °C) with an external heating/cooling bath and was monitored by a thermocouple that extended into the polymerization vessel. Solutions of MAO (500 equiv) and catalyst precursor in toluene were sequentially injected. The mixture was stirred for 3 min at a rate of 150 rpm after each addition. The rate of stirring was increased to 1000 rpm, and the vessel was vented of N_2 and pressurized with ethylene (33 psi). Any exotherm was within the allowed temperature differential of the heating/cooling system. The solution was stirred for 1 h, after which time the reaction was quenched with 1 M HCl in MeOH. The precipitated polymer was subsequently washed with MeOH and dried at 100 °C for at least 24 h prior to weighing.

X-ray Data Collection and Reduction. X-ray quality crystals were obtained as described above. The crystals were manipulated and mounted in capillaries in a glovebox, thus maintaining a dry, O_2-free environment for each crystal. Diffraction experiments were performed on a Siemens SMART System CCD diffractometer. In the later case the data were collect in a hemisphere of data in 1329 frames with 10 s exposure times. Crystal data are summarized in Table 1. The observed extinctions were consistent with the space groups in each case. The data sets were collected ($4.5° < 2\theta < 45-50.0°$). A measure of decay was obtained by re-collecting the first 50 frames of each data set. The intensities of reflections within these frames showed no statistically significant change over the duration of the data collections. The data were processed using the SAINT and XPREP processing package. An empirical absorption correction based on redundant data was applied to each data set. Subsequent solution and refinement was performed using the SHELXTL solution package operating on a Pentium computer.

Structure Solution and Refinement. Non-hydrogen atomic scattering factors were taken from the literature tabulations.[17] The heavy atom positions were determined using direct methods employing either the SHELXTL or direct methods routines. The remaining non-hydrogen atoms were located from successive difference Fourier map calculations. The refinements were carried out by using full-matrix least squares techniques on *F*, minimizing the function $w(|F_o| - |F_c|)^2$, where the weight *w* is defined as $4F_o^2/2\sigma(F_o^2)$ and F_o and F_c are the observed and calculated structure factor amplitudes. In the final cycles of each refinement, all non-hydrogen atoms were assigned anisotropic temperature factors. Carbon-bound hydrogen atom positions were calculated and allowed to ride

(17) Cromer, D. T.; Mann, J. B. *Acta Crystallogr. A* **1968**, *A24*, 321−324.

Table 2. Polymerization Data[a]

catalyst/cocatalyst	temp (°C)	time (min)	activity (g PE/mmol·h·bar)	M_w ($\times 10^{-3}$)[e]	PDI[e]	mp
slurry polymerization						
3/MAO/$Ph_3C[B(C_6F_5)_4]$[b]	83.1	24	55	139.6	1.7	136.2
2/MAO	51.5	30	2	480.3	11.3	132.1
slurry copolymerization						
3/MAO[c]	51.2	15	5	509.9	7.0	106.7
5/MAO[c]	50.0	30	0.3	468.8	16.7	125.3
solution polymerization						
3/MAO/$Ph_3C[B(C_6F_5)_4]$[d]	158.5	10	49	451.1	1.82	133.9
5/MAO/$Ph_3C[B(C_6F_5)_4]$[d]	159.2	10	13	547.1	1.71	141.5

[a] General polymerization conditions: 300 psig C2; 300 umol/L of catalyst; Al/Fe = 60; 216 mL of toluene; MAO at 1 mmol/L as a scavenger. [b] Al/Fe = 20; B/Al = 1.05. [c] As above with 100 psig C2; 30 mL of 1-octene; 216 mL of toluene. [d] 200 psig C2; 200 umol/L of catalyst; Al/Fe = 20; B/Al = 1.05; PMAO at 1 mmol/L as a scavenger; 216 mL of toluene. [e] Molecular weights and PDI were measured by GPC at 140 °C in 1,2,4-trichlorobenzene calibrated using polyethylene standards.

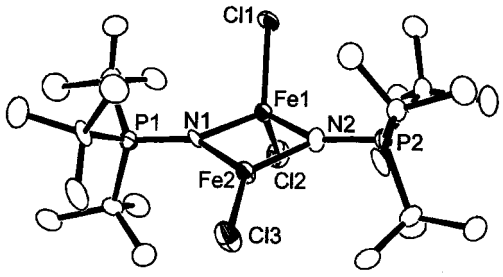

Figure 1. ORTEP drawing of **1**; 20% thermal ellipsoids are shown. Hydrogen atoms are omitted for clarity. Fe(1)−N(1) 1.912(9), Fe(1)−N(2) 1.927(8), Fe(1)−Cl(1) 2.242(4), Fe(1)−Cl(2) 2.244(4), Fe(1)−Fe(2) 2.523(2), Fe(2)−N(1) 1.933(8), Fe(2)−N(2) 1.948(10), Fe(2)−Cl(3) 2.211(3), P(1)−N(1) 1.626(9), N(1)−Fe(1)−N(2) 99.0(4), N(1)−Fe(1)−Cl(1) 110.1(3), N(2)−Fe(1)−Cl(1) 110.1(3), N(1)−Fe(1)−Cl(2) 113.6(3), N(2)−Fe(1)−Cl(2) 110.5(3), Cl(1)−Fe(1)−Cl(2) 112.78(16), N(1)−Fe(2)−N(2) 97.5(4), N(1)−Fe(2)−Cl(3) 130.7(3), N(2)−Fe(2)−Cl(3) 131.7(3), P(1)−N(1)−Fe(1) 142.5(5), P(1)−N(1)−Fe(2) 135.4(5), Fe(1)−N(1)−Fe(2) 82.0(3), P(2)−N(2)−Fe(1) 142.8(6), P(2)−N(2)−Fe(2) 136.0(5), Fe(1)−N(2)−Fe(2) 81.3(3).

on the carbon to which they are bonded assuming a C−H bond length of 0.95 Å. Hydrogen atom temperature factors were fixed at 1.10 times the isotropic temperature factor of the carbon atom to which they are bonded. The hydrogen atom contributions were calculated, but not refined. The final values of refinement parameters are given in Table 1. The locations of the largest peaks in the final difference Fourier map calculation as well as the magnitude of the residual electron densities in each case were of no chemical significance. Crystallographic information files have been deposited as Supporting Information.

Results and Discussion

A solution of Li[NP*t*-Bu_3] in THF was added to a suspension of $FeCl_2$ in THF and allowed to react for 2 h at room temperature, affording a dark solution with a gray-colored precipitate. Removal of the solvent under vacuum and replacement with CH_2Cl_2 resulted in the subsequent isolation of red crystals of **1** in 71% yield. X-ray crystallographic study of **1** established the formulation as $[Cl_3Fe_2(\mu\text{-NP}t\text{-Bu}_3)_2]$ (Figure 1), in which two phosphinimide ligands bridge two inequivalent iron centers. The Fe_2N_2 core is planar with Fe−N distances in the range 1.912(9)−1.948(10) Å, while the Fe−Fe separation is 2.523(2) Å. One of the iron centers, Fe(1) is pseudo-tetrahedral with two chloride ions completing the coordination sphere with an average Fe−Cl distance of 2.243(4) Å. The second iron center adopts a pseudo-trigonal planar coordination sphere comprised of the two phosphinimide nitrogens and a single chloride ion. The Fe−Cl distance in this case is 2.211(3) Å. This structure confirms a mixed valent Fe(III)−Fe(II) formulation consistent with the intermediate effective magnetic moment of 2.60 μ_B.

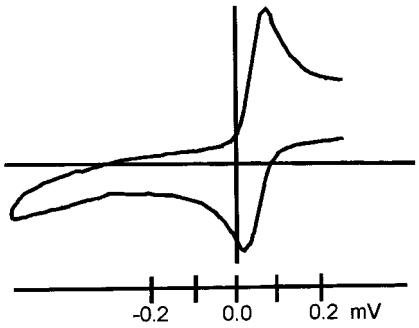

Figure 2. Cyclic voltammetry of **1** in CH_2Cl_2 with $[Bu_4N]PF_6$ as the supporting electrolyte. The vertical axis denotes 0.0 V relative to SCE.

It is noteworthy that all efforts to isolate a purely Fe(II) species were unsuccessful. In contrast, Dehnicke and co-workers have described the Fe(II) tetrameric aggregate $[ClFe(\mu\text{-NPEt}_3)]_4$ with a cubane type structure. Dehnicke et al.[18] have also reported that use of the more sterically demanding phosphinimide ligand $[(Me_2N)_3PN]^-$ precludes tetramer formation, affording instead the mixed-valent trimetallic species $[Fe_3Cl_4(NP(NMe_2)_3)_3]$.[18] In the present work, the even greater steric demand of the phosphinimide ligand $[t\text{-Bu}_3PN]^-$ presumably precludes aggregation to analogous tetramers or trimers, prompting disproportionation and formation of the mixed valent dimeric species **1**.

The presence of a coordinatively unsaturated Fe center in the Fe(III)/Fe(II) dimer **1** prompted attempts to bind other ancillary donors such as olefins, nitriles, isonitriles, and phosphines to the tricoordinate Fe center. No evidence of ligand coordination was observed. The redox properties of **1** were probed via cyclic voltammetry in CH_2Cl_2 employing $[Bu_4N]PF_6$ as the supporting electrolyte and a Pt electrode. A reversible one-electron redox process is observed centered at 90 mV versus the SCE, consistent with a one-electron oxidation of **1** to $[Cl_3Fe_2(\mu\text{-NP}t\text{-Bu}_3)_2]^+$ (Figure 2, Scheme 1). Application of reducing potentials showed no evidence of the reduction of **1** prior to the reduction of the solvent.

(18) Riese, U.; Harms, K.; Pebler, J.; Dehnicke, K. *Z. Anorg. Allg. Chem.* **1999**, *625*, 746−754.

Scheme 1

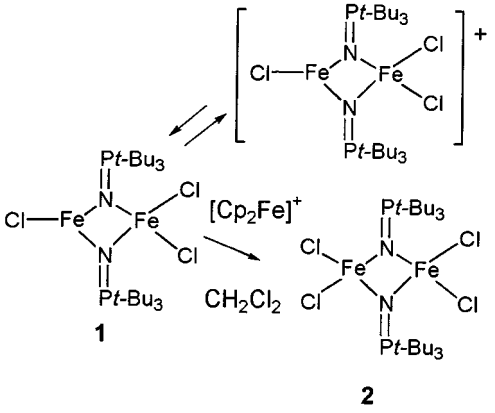

Scheme 2

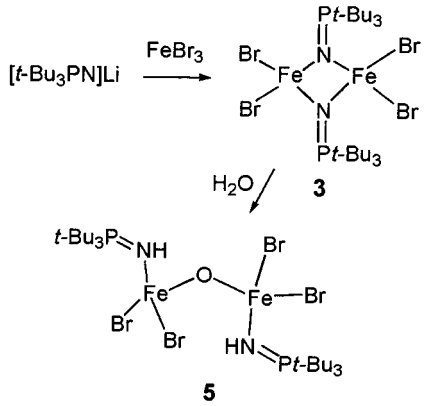

This infers that CH_2Cl_2 would act to oxidize an Fe(II)−Fe(II) species, an observation that may account for the isolation of partial oxidation product **1** from the preparation described above. Attempts to intercept the cationic Fe(III)/Fe(III) dimer with donor ligands also proved unsuccessful.

Reaction of **1** with $[Cp_2Fe]PF_6$ was performed in CH_2Cl_2. Stirring for 2 h resulted in the generation of a red-brown solution. The solvent was removed, and the residue washed with hexane and crystallized from CH_2Cl_2 to give a new species, **2**, in 90% yield. X-ray crystallographic characterization of **2** established the formulation as $[Cl_2Fe(\mu\text{-}NPt\text{-}Bu_3)]_2$ (Figure 3a). Crystallographic symmetry imposes mirror symmetry on the dimeric structure. Thus, one of the *tert*-butyl groups and the P and N atoms sit precisely on the mirror plane. Two chloride ions complete each of the coordination spheres of the symmetry-related Fe centers. The Fe−N and Fe−Cl distances average 1.933(4) and 2.2340(18) Å respectively. The Fe_2N_2 core is similar to that seen in **1** with a slightly larger Fe−Fe separation of 2.5659(13) Å. The compound **2** was found to have an effective magnetic moment of 4.11 μ_B, consistent with the Fe(III)/Fe(III) formulation.

On the basis of the electrochemical properties of **1** and the characterization of **2**, it appears that $[Cl_3Fe_2(\mu\text{-}NPt\text{-}Bu_3)_2]^+$ abstracts a chloride from CH_2Cl_2, resulting in the formation of **2**. Attempts to develop a direct synthesis of **2** via reaction of $FeCl_3$ with either $Li[NPt\text{-}Bu_3]$ or $Me_3SiNPt\text{-}Bu_3$ proved unsuccessful, yielding only oily, uncharacterized products. In contrast, reaction of $Li[NPt\text{-}Bu_3]$ in hexane with $FeBr_3$ in toluene gave an orange crystalline product **3** in 96% yield. The product was formulated as $[Br_2Fe(\mu\text{-}NPt\text{-}Bu_3)]_2$ **3** by analogy with the crystallographically characterized species **2**. The analogous reaction of $FeCl_3$ with $Me_3SiNPCy_3$ affords the red-brown species **4** in modest yields. The compound **4** was also shown to be a crystallographically centrosymmetric dimer, generally analogous to **3** (Figure 3b). It is noteworthy that the Fe−N distance in **4** is significantly longer than those found in **2** and the analogous species $[Cl_2Fe(\mu\text{-}NPR_3)]_2$ (R = Ph, Et) previously described by groups of Roesky and Dehnicke.[19,20] This, again reflects the greater steric demands of the phosphinimide ligand $[t\text{-}Bu_3PN]^-$.

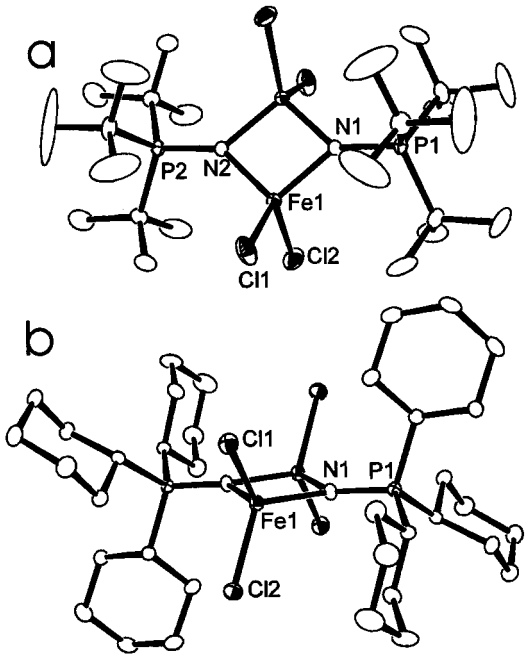

Figure 3. ORTEP drawings of (a) **2** and (b) **4**; 20% thermal ellipsoids are shown. Hydrogen atoms are omitted for clarity. **2**: Fe(1)−N(2) 1.927(4), Fe(1)−N(1) 1.940(4), Fe(1)−Cl(1) 2.2260(17), Fe(1)−Cl(2) 2.2421(18), Fe(1)−Fe(1′) 2.5659(13), P(1)−N(1) 1.642(5), N(2)−Fe(1)−N(1) 96.71(15), N(2)−Fe(1)−Cl(1) 115.60(16), N(1)−Fe(1)−Cl(1) 115.38(15), N(2)−Fe(1)−Cl(2) 108.34(17), N(1)−Fe(1)−Cl(2) 111.00(17), Cl(1)−Fe(1)−Cl(2) 109.19(9). P(1)−N(1)−Fe(1) 138.56(10), P(1)−N(1)−Fe(1) 138.56(10), Fe(1)−N(1)−Fe(1) 82.8(2), P(2)−N(2)−Fe(1) 138.24(11), P(2)−N(2)−Fe(1) 138.24(11), Fe(1)−N(2)−Fe(1) 83.5(2). **4**: Fe(1)−N(1) 1.909(4), Fe(1)−N(1)′ 1.922(4), Fe(1)−Cl(1) 2.2227(16), Fe(1)−Cl(2) 2.2281(16), Fe(1)−Fe(1)′ 2.6133(15), P(1)−N(1) 1.619(4), N(1)−Fe(1)−N(1)′ 93.98(16), N(1)−Fe(1)−Cl(1) 113.81(14), N(1)′−Fe(1)−Cl(1) 112.14(14), N(1)−Fe(1)−Cl(2) 115.49(13), N(1)′−Fe(1) Cl(2) 110.09(13), Cl(1)−Fe(1)−Cl(2) 110.35(7), P(1)−N(1)−Fe(1) 141.8(3), P(1)−N(1)′−Fe(1) 131.7(2), Fe(1)−N(1)−Fe(1) 86.02(16).

In some attempts to prepare **4** it was uncovered that inferior quality (i.e., slightly wet) commercial-grade $FeBr_3$ led to the formation of a light green powder **5**. This same green material could be deliberately synthesized directly from **4** via addition of an equivalent of H_2O. This product of hydrolysis **5** was identified by single-crystal X-ray crystallography as species $[(t\text{-}Bu_3\text{-}$

(19) Roesky, H. W.; Seseke, U.; Noltemeyer, M.; Sheldrick, G. M. *Z. Naturforsch.* **1988**, *43b*, 1138.
(20) Mai, H. J.; Wocadlo, S.; Kang, H. C.; Massa, W.; Dehnicke, K.; Maichle-Moessmer, C.; Straehle, J.; Fenske, D. *Z. Anorg. Allg. Chem.* **1995**, *621*, 705−712.

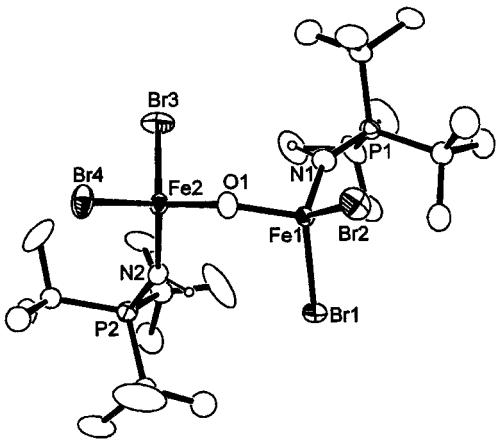

Figure 4. ORTEP drawings of **5**; 20% thermal ellipsoids are shown. Hydrogen atoms are omitted for clarity. Fe(1)−O(1) 1.768(7), Fe(1)−N(1) 1.908(9), Fe(1)−Br(1) 2.3698(18), Fe(1)−Br(2) 2.3704(17), P(1)−N(1) 1.630(9), O(1)−Fe(2) 1.760(7), Fe(2)−N(2) 1.950(7), Fe(2)−Br(4) 2.3548(18), Fe(2)−Br(3) 2.363(2), P(2)−N(2) 1.604(8), O(1)−Fe(1)−N(1) 101.9(4), O(1)−Fe(1)−Br(1) 109.2(3), N(1)−Fe(1)−Br(1) 114.7(3), O(1)−Fe(1)−Br(2) 105.7(2), N(1)−Fe(1)−Br(2) 113.4(3), Br(1)−Fe(1)−Br(2) 111.02(7), P(1)−N(1)−Fe(1) 150.3(6), O(1)−Fe(2)−N(2) 104.8(3), O(1)−Fe(2)−Br(4) 105.8(3), N(2)−Fe(2)−Br(4) 112.5(2), O(1)−Fe(2)−Br(3) 107.5(3), N(2)−Fe(2)−Br(3) 113.4(3), Br(4)−Fe(2)−Br(3) 112.17(8), P(2)−N(2)−Fe(2) 148.9(5).

PNH)Br_2Fe]$_2$(μ-O) **5** (Figure 4). The Fe−O distances in this oxo-bridged diiron complexes average 1.764(7) Å, while the Fe−O−Fe′ angle is 148.1(5)°. The Fe−N distances average 1.929(9) Å, and the Fe−Br distances range from 2.3548(18) to 2.3704(17) Å. The angles about both Fe centers are consistent with slightly distorted tetrahedral coordination spheres.

Ethylene Polymerization. The ability of these Fe species to effect ethylene polymerization catalysis in solution and slurry phase was probed using a 500 mL Autoclave reactor equipped with an air-driven stirrer and an automatic temperature control system. All solvent, catalyst (200 umol/L), and cocatalyst were fed into the reactor batchwise except ethylene, which was fed on demand at 200 psig. Reactions were terminated by the addition of methanol (5 mL), and the polymer was recovered by solvent removal. Results of preliminary screening of these species in slurry polymerization at 50 °C revealed that activation of compound **3** with a combination of MAO and $Ph_3C[B(C_6F_5)_4]$ afforded a single-site ethylene polymerization catalyst (55 g PE/mmol Fe·h/bar). The resulting polymer has a M_w of 139 000 with a polydispersity index of 1.7. Activation of compound **2** by MAO alone results in much lower activity and a polymer with much higher polydispersity, suggesting the generation of multiple low-activity sites. Analogous slurry copolymerization of ethylene/1-octene using **3**/MAO generated polymer with octene incorporation with 1.7 branches/1000 carbons, as evidenced by $^{13}C\{^1H\}$ NMR data.

Solution polymerization was also performed at 160 °C and 200 psig of ethylene. Consistent with the best results in slurry polymerizations, a combination of MAO and $Ph_3C[B(C_6F_5)_4]$ was used to effect activation. The ratios of Al/Fe and B/Fe were 20 and 1.05, respectively. Compound **3** yields an active single-site catalyst for the polymerization of ethylene giving 49 g PE/mmol Fe·h/bar. The resulting polymer had a M_w of 451 000 with a PDI of 1.82, consistent with single-site character. It is noteworthy that the Fe-catalyst derived from [(C_5H_3N)-(CR=NC_6H_3*i*-Pr_2)$_2$]$FeBr_2$/MAO[5,9] degrades under these conditions. Although it generates 53 g PE/mmol Fe·h/bar (287 psig, 140 °C, M_w 457 000), the polydispersity is very broad (PDI = 48) under these more demanding conditions.

In what is perhaps a surprising observation, compound **5** also affords an active single-site catalyst in solution polymerization, producing 13 g PE//mmol Fe·h/bar. The resulting polymer is similar to that produced from **3** with a M_w of 547 100 and a polydispersity index of 1.71. Although the nature of the active species derived from these two precursors has not been unambiguously identified, the similarity of the products derived from **3** and **5** and the single site behavior suggest the possibility that MAO dehydrates **5**, generating a catalyst similar to that derived from **3**. This suggests that compounds thought to be products of deactivation may be worthy of further study. The development of related but more active catalyst precursors is the target of ongoing efforts.

Acknowledgment. Financial support from NSERC of Canada and NOVA Chemicals is gratefully acknowledged.

Supporting Information Available: Crystallographic data. This material is available free of charge via the Internet at http://pubs.acs.org.

OM011041M